Solid and liquid carbon monoxide studied with the use of constant-pressure molecular dynamics

Pier Francesco Fracassi*
Institute for Materials Research, McMaster University, Hamilton, Ontario, Canada L8S 4M1

Gianni Cardini* and Séamus O'Shea
Department of Chemistry, University of Lethbridge, Lethbridge, Alberta, Canada T1K 3M4

Roger W. Impey and Michael L. Klein
Chemistry Division, National Research Council of Canada, Ottawa, Canada K1A 0R6
(Received 9 September 1985)

Constant-pressure molecular-dynamics calculations have been carried out for the zero-pressure condensed phases of carbon monoxide using an intermolecular potential based on previous lattice-dynamics calculations. We have explored the nature of phonons in the low-temperature cubic α phase and the properties of the hexagonal plastic phase and the liquid. The proposed potential model accounts for the dynamics of the α phase and gives a semiquantitative description of the phase diagram of condensed CO.

I. INTRODUCTION

Lattice dynamics is one of the basic techniques used to study the behavior of classical solids. Recent advances have led to sophisticated treatments of complex molecular crystals and ionic salts with molecular anions and cations.[1-3] However, the treatment of orientationally disordered solids remains a difficult problem even for semi-analytical theories.[4-6] A useful complementary approach is provided by molecular dynamics.[7-9] Such calculations can be used to study ordered solids, and can equally be applied to disordered (plastic) phases and liquids. In conventional molecular dynamics (MD), the Newtonian equations of motion are integrated numerically for a system of N molecules, interacting with a specific intermolecular potential and confined to a fixed volume V. Quite recently, Andersen proposed how one might carry out MD calculations on liquids under conditions of constant pressure and/or constant temperature.[10] A generalization of the Andersen (NPH) ensemble MD technique to handle solids was introduced by Parrinello and Rahman.[11,12] They allowed the MD cell to change its shape as well as its volume. This development was particularly important for the study of phase transformations in molecular solids.[13] Both the lattice-dynamics[1-3] and MD methods,[7-13] and their applications to molecular systems, are well documented in the literature, so we omit most of the details here.

Although complex systems have been studied by MD methods with a certain degree of success,[14] there is also renewed interest in smaller molecules, whose intermolecular potentials continue to pose problems.[15-18] In this respect, carbon monoxide is a system worthy of further study. Recently, we proposed an intermolecular potential for CO which was based in part on theoretical and experimental studies of the CO molecule.[19-23] The potential was arrived at by making extensive use of both harmonic and anharmonic lattice-dynamics calculations on a hypothetical orientationally ordered α phase with a $P2_13$ structure. Since the agreement with measured infrared and Raman frequencies was rather good, it seemed instructive to use the potential in a MD study of the disordered β phase and the liquid.

Preliminary constant-volume MD simulations, performed using a MD cell of only 32 molecules, showed that the potential model[19] was able to account for a stable ordered cubic α phase. This finding convinced us to embark on the more extensive series of constant-pressure MD calculations reported here. Thus we provide a more complete dynamical study not only of the cubic α phase, but also the hexagonal plastic phase and the liquid. The paper is structured as follows. In the next section we review the properties of condensed CO. Then, in Sec. III the intermolecular potential of Ref. 19 is described. The MD calculations and results are detailed in Secs. IV and V.

II. PROPERTIES OF CONDENSED CARBON MONOXIDE

At low pressure condensed CO exists in two solid allotropes.[24-27] At temperatures below 61.5 K it is a cubic crystal (α-CO) with the molecules aligned along the $\langle 111 \rangle$ body diagonals.[28,29] The residual entropy detected in calorimetric measurements[24,25] is evidence of random head-to-tail disorder of the molecules (a finding which is confirmed by recent dielectric,[30] (NQR),[31,32] and NMR[33] measurements). The kinetics of the molecular reorientation in the cubic phase has also been discussed. Reordering of the molecules via quantum tunneling was ruled out,[34] and the extremely low dipolar ordering temperature (5 K, according to Ref. 35) implies that the cubic phase is

likely to exist with nonequilibrium short-range order.[27,32] It is therefore convenient to carry out calculations on a fully ordered antiferroelectric structure[19,36] which belongs to the group $P2_13$ (T^4). There are four molecules per cubic unit cell, and the C and O atoms occupy sites of type a. The distortion $s=\sqrt{3}(x_O+x_C)$ from the centrosymmetric $Pa3$ structure is rather small. In Ref. 19 we found that the potential described in the next section yields a minimum of the static lattice energy with $x_C=-0.0513a_0$ and $x_O=0.0641a_0$ and hence the distortion $s=0.022a_0$, where a_0 is the cubic lattice constant. In this fully ordered structure there are three Raman-active $\mathbf{k}=0$ lattice modes (one translation with symmetry A, and two mixed translation-libration modes with symmetry E), and four mixed modes which are both infrared and Raman active (all four with symmetry F). Both the infrared[37,38] and Raman[39] spectra for the lattice-mode region have been reported.

Between 61.5 and 68.1 K carbon monoxide is an hexagonal-close-packed crystal (β-CO) belonging to the space group $P6_3/mmc$ (D_{6h}^4),[28] with two molecules per unit cell and a c/a ratio of 1.624.[29] The α-β transition is characterized by an enthalpy change of 0.628 kJ mol^{-1},[25] and an increase in the molar volume of about 1×10^{-3} cm^3 mol^{-1}.[29,40] The elastic constants of β-CO have been measured using Brillouin scattering.[41] Also, self-diffusion of CO molecules due to migration of monovacancies has also been detected.[42] As in the case of β-N_2, β-CO is a plastic crystal in which the molecules undergo rotational diffusion. This motion is likely *not* quasifree precessional motion about the c axis.[43]

At 68.1 K carbon monoxide melts with a heat of fusion of 0.829 kJ mol^{-1}.[25,44] The density of the liquid at various temperatures is also known.[45] NMR and NQR studies[31,40] studies have been made of the molecular diffusion in liquid CO and the behavior is virtually identical to that of liquid N_2.

III. THE POTENTIAL MODEL

The intermolecular potential used in the present MD calculations is the same as described in Ref. 19. The molecular bond length is 1.128 Å.[46] Three point charges are placed on each molecule with magnitudes and positions given, respectively, by $(-0.636|e|, -1.0820$ Å), $(0.831|e|, -0.6446$ Å), and $(-0.195|e|, 0.3256$ Å). Here charges are expressed in units of the electron charge and positions are given with respect to the molecular center of mass. The atomic sites, in the same coordinate system, are located at -0.6446 Å (C) and 0.4834 Å (O). These sites, together with the center of mass (c.m.), are used to specify the dispersion and the exchange forces by means of a site-site potential of the form

$$V^{\alpha\beta}(R)=A^{\alpha\beta}\exp(-B^{\alpha\beta}R)-F(R)(C_6^{\alpha\beta}/R^6+C_8^{\alpha\beta}/R^8+C_{10}^{\alpha\beta}/R^{10}),$$
$$F(R)=1,\quad R\le R^{\alpha\beta} \tag{1}$$
$$F(R)=\exp[-(R-R^{\alpha\beta})^2/R^2],\quad R\le R^{\alpha\beta}$$

with α,β=C, O, c.m. The parameters characterizing the interactions are listed in Table I. Lattice-dynamics results for this potential are given in Table II. The final form of the potential was arrived at by optimizing the static lattice energy and the Raman- and the infrared-active phonon frequencies of the α phase.[19] Most of the lattice normal modes show both librational and translational components, which indicates the overall importance of the translation-rotation coupling. However, the high-frequency modes are mostly librational, and the low-frequency ones are more translational in character. In particular, the mixing of the lowest E mode with the transverse-acoustic branches lead to anomalous acoustic dispersion in the $\langle 110\rangle$ direction of the Brillouin zone.[19]

The experimental sublimation energy[47] is -8.30 kJ/mol, and at the experimental lattice constant ($a_0=5.644$ Å) the potential described above yields the value -8.14 kJ/mol, of which -7.80 kJ/mol is due to the atom-atom potential, -2.40 kJ/mol to the electrostatic interactions, and 2.06 kJ/mol to the zero-point energy.

IV. MOLECULAR-DYNAMICS CALCULATIONS

The constant-pressure MD calculations were performed on a Cray-1S using a fourth-order quaternion and third-order predictor-corrector algorithms.[48–50] The single-particle time-dependent properties for the α phase were obtained from constant-volume MD calculations performed on a DEC-20 system, using the Verlet algorithm with the atoms-plus-constraint method.[51]

The constant-pressure calculations[50] were initiated by arranging CO molecules in the fully ordered $P2_13$ structure.[36] The cubic MD cell contained 108 molecules. As usual, periodic boundary conditions were employed, and the temperature was adjusted by scaling the linear and angular velocities. The equations of motion were integrated using a time step of 2×10^{-15} s.

At first, a constant-volume equilibration run of 6 ps was performed at a temperature of 30 K. Each subsequent constant-pressure run[13] included an equilibration

TABLE I. Intramolecular potential parameters for CO taken from Ref. 19 in units of kJ/mol and Å (c.m. denotes center of mass).

α-β	$A^{\alpha\beta}$	$B^{\alpha\beta}$	$C_6^{\alpha\beta}$	$C_8^{\alpha\beta}$	$C_{10}^{\alpha\beta}$	$R^{\alpha\beta}$
C-C	367 271.0	3.269	3298.0	27654.0	247 853.0	3.55
C-O	289 465.0	3.512	0.0	0.0	0.0	
C-c.m.	−87 587.0	3.113	0.0	0.0	0.0	
O-O	352 959.0	3.505	0.0	0.0	0.0	
O-c.m.	−161 878.0	3.333	0.0	0.0	0.0	
c.m.-c.m.	30 305.0	2.971	1383.0	9480.0	103 701.0	4.45

TABLE II. Zero-wave-vector modes for the ordered $P2_13$ structure solid CO in units of cm^{-1}.

Mode[a]	Symmetry	Ω_{harm}[b]	Ω_{anharm}[b]	$2\Gamma_{anharm}$	Ω[c]	2Γ[c]
L	F	114.6	115.8	22.0	90.5	7
LT	F	84.9	82.2	9.6	85	12
LT	E	72.7	76.3	8.6	64.5	
LT	F	59.2	65.5	13.4	58	
T	A	48.3	48.7	2.6		
T	F	46.4	46.7	8.0	52,49	5,7
T	E	43.4	43.7	7.7	44	

[a]L (libration), T (translation), and LT (mixed libration-translation).
[b]Reference 19.
[c]References 37–39.

TABLE III. MD results for the cubic α phase of solid CO. Averages taken over the 2000 time steps of each production run. E is the total energy and U is the mean configurational energy. The lattice constants (a,b,c) and angles (α,β,γ) refer to the crystal unit cell.

	Run			
	1	2	3	4
T (K)	30.97	41.56	45.87	53.28
P (kbar)	−0.14	−0.12	−0.11	−0.07
V (cm^3/mol)	26.66	27.20	27.47	28.64
E (kJ/mol)	−8.69	−8.13	−7.88	−7.13
U (kJ/mol)	−9.33	−9.00	−8.83	−8.24
H (kJ/mol)	−7.62	−7.04	−6.77	−5.97
a (Å)	5.60±0.03	5.65±0.03	5.66±0.06	5.69±0.10
b (Å)	5.62±0.04	5.65±0.02	5.68±0.05	5.78±0.09
c (Å)	5.61±0.02	5.65±0.04	5.66±0.03	5.77±0.07
α (deg)	89.0±0.4	89.9±0.3	89.9±0.3	90.4±0.8
β (deg)	90.0±0.3	89.9±0.5	90.0±0.5	90.6±0.7
γ (deg)	90.0±0.2	90.0±0.5	90.0±0.5	91.3±1.6

TABLE IV. MD results for liquid CO (see caption in Table III).

	Run				
	5	V	6	7	8
T (K)	61.35	71.15	75.81	88.34	94.66
P (kbar)	0.01	−0.04	0.06	0.07	0.11
V (cm^3/mol)	30.25	32.14	32.24	33.61	35.08
E (kJ/mol)	−6.52	−5.85	−5.57	−4.90	−4.45
U (kJ/mol)	−7.93	−7.33	−7.15	−6.73	−6.42
H (kJ/mol)	−5.34	−4.75	−4.17	−3.44	−2.93
D (10^{-5} cm^2/sec)	1.0±0.3	1.9±0.6	4.3±1.3	5.4±1.6	6.2±1.8

TABLE V. MD results for the hexagonal β phase of solid CO (see caption in Table III).

	Run			
	I	II	III	IV
T (K)	42.96	53.26	55.73	60.93
P (kbar)	−0.12	−0.10	−0.09	−0.08
V (cm^3/mol)	29.37	29.86	29.89	30.62
E (kJ/mol)	−7.59	−7.15	−7.14	−6.68
U (kJ/mol)	−8.40	−8.26	−8.26	−7.94
H (kJ/mol)	−6.72	−6.13	−6.11	−5.68
a (Å)	4.07±0.04	4.31±0.06	4.18±0.04	4.45±0.05
b (Å)	4.18±0.03	4.04±0.03	4.10±0.04	4.20±0.05
c (Å)	6.62±0.05	6.71±0.04	6.68±0.05	6.51±0.07
α (deg)	90.76±1.2	93.2±1.8	88.1±1.1	86.3±1.9
β (deg)	90.5±0.9	90.2±1.3	89.5±0.9	91.9±1.8
γ (deg)	118.6±0.4	121.8±0.3	120.0±0.7	123.3±1.3

phase of 1000 time steps and a production phase of 2000 time steps. The value of the external pressure P_{ext} was always chosen with due consideration of the contribution to the pressure arising from the truncated tails of the electrostatic and atom-atom potentials. Throughout, the kinetic energy associated with variations in shape of the MD cell was calculated using a mass parameter roughly equal to the mass of one CO molecule.[10] We used a cutoff radius for the site-site potentials of 7 Å, but an Ewald sum was used for the electrostatic interactions. Starting from the ordered $P2_13$ configuration at 30 K, the temperature was increased in stages to 94 K, while keeping the total pressure $P \approx 0$ kbar. The results are contained in Tables III and IV.

The hexagonal rotator phase was equilibrated with a constant-volume MD run at $T=39$ K, the hexagonal MD cell containing 128 molecules. Then, constant-pressure MD runs were performed with $P \approx 0$ kbar, in an analogous fashion to those for the cubic phase but for temperatures up to 71 K. The simulation data are presented in Tables IV and V.

Two constant-volume MD runs were also performed at 30 and 5 K on the fully ordered antiferromagnetic structure, using a time step of 5×10^{-15} s. Here an equilibration stage of 2000 time steps was followed by production runs of 8200 time steps.

V. RESULTS

The molar volume corresponding to each MD run is compared with experimental data in Fig. 1, and the calculated enthalpies are plotted in Fig. 2. In both figures Roman numerals are used to denote runs initiated from an hexagonal structure while Arabic numerals label those initiated from a cubic structure. The inset of Fig. 1 is the measured heat capacity of CO, which is used to indicate the experimental transition temperatures.

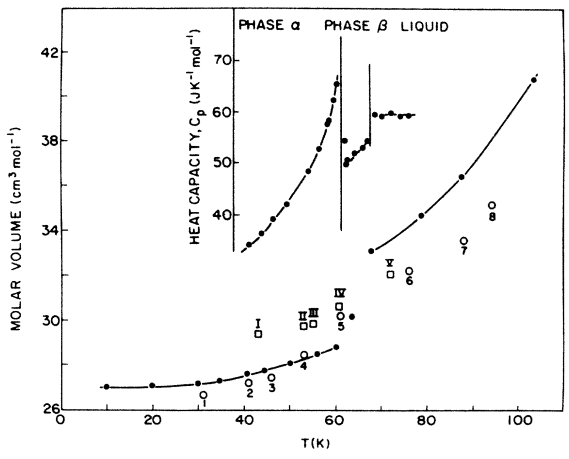

FIG. 1. Temperature dependence of the molar volume and heat capacity of CO under its own vapor pressure. The solid circles are the experimental data from Refs. 24, 29, and 45. The open circles (labeled with Arabic numerals) are the constant-pressure MD results for the $P2_13$ structure and the liquid, while the squares (labeled with Roman numerals) refer to the MD results for the hcp structure (see the text).

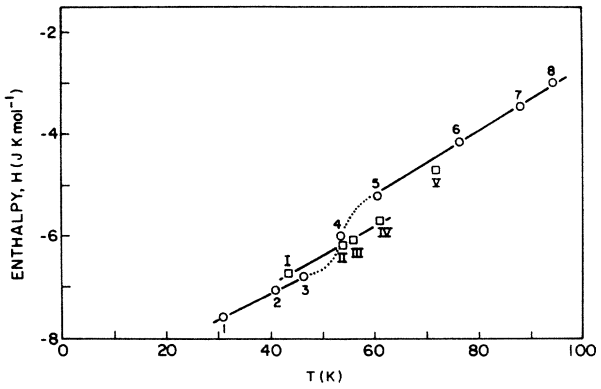

FIG. 2. Temperature dependence of the enthalpy of CO as derived from constant-pressure MD calculations. The open circles (labeled with Arabic numerals) refer to the $P2_13$ structure and the liquid, while the squares (labeled with Roman numerals) refer the hcp structure (see the text).

A. Stability of the Cubic phase

Figure 3 shows $g_{\alpha\beta}(R)$, the angle-averaged atom-atom distribution function obtained from the MD run of Table III at $T=31$ K. The coordination numbers obtained by integrating the areas under the peaks of $g_{00}(R)$ reproduce the value (i.e., 6) expected in a static $P2_13$ structure. Similar results are obtained from the carbon-carbon and carbon-oxygen distributions. The $g(R)$'s clearly show that the proposed potential yields a stable ordered $P2_13$ structure for the cubic phase of solid CO. This structure

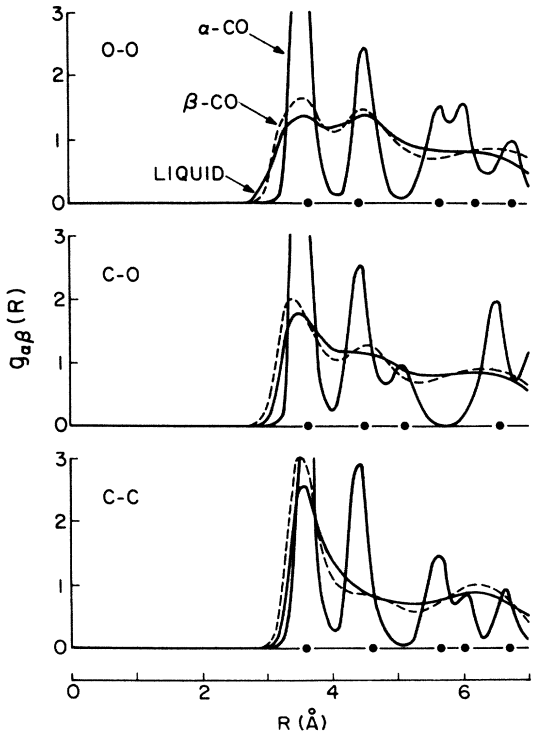

FIG. 3. Angle-averaged atom-atom distribution functions $g_{\alpha\beta}(R)$ for CO in the ordered solid (phase α), the plastic solid (phase β), and the liquid (see the text). The dots refer to the positions of the peaks in a static $P2_13$ structure.

is substantially preserved for temperatures up to 53 K (run 4 in Table III), where thermal motion starts blurring the distinction between the fourth and fifth peaks in $g(R)$. In run 5 of Table IV at $T=61$ K, the cubic structure was no longer stable: certain peaks in the radial distribution functions merge and the MD cell continually deforms with large fluctuations, which we interpret as the onset of the melting process. We found no evidence of a transition towards the hexagonal plastic phase.

B. Dynamics of the cubic phase

The two constant-volume MD runs mentioned above were used to calculate the dynamical structure factor

$$S(\mathbf{k},\omega)=\int \langle \rho(\mathbf{k},t)\rho(-\mathbf{k},0)\rangle \exp(-i\omega t)dt \ , \tag{2}$$

where $\rho(\mathbf{k},t)$ is the wave-vector-dependent density function defined by

$$\rho(\mathbf{k},t)=\sum_i \exp[i\mathbf{k}\cdot\mathbf{r}_i(t)] \ . \tag{3}$$

The angular brackets denote an average over time origins and $\mathbf{r}_i(t)$ is the instantaneous position of the ith atom. $S(\mathbf{k},\omega)$ is directly related to the spectrum of coherent neutron scattering measurements. The peaks in $S(\mathbf{k},\omega)$ calculated from the MD data at the Γ point of the Brillouin zone are reported in Table VI, where they are compared with previous lattice-dynamics calculations[19] and experimental data.[37–39] Figure 4 shows Raman spectra evaluated from the MD results at 5 K. The spectrum was obtained by first constructing the time correlation function describing the relaxation of the anisotropic part of the molecular polarizability in the crystal frame, and then evaluating its Fourier transform. The appropriate time correlation functions have the form

$$R(t)=\left\langle \sum_l A_l(t) \sum_m A_m(0) \right\rangle , \tag{4}$$

TABLE VI. Phonon frequencies (in cm^{-1}) for α-CO at the Γ point.

Mode	LD[a]	MD_S[b]	MD_{Raman}[c]	Expt.[d]
F	115.8	114	114	90.5
F	82.2	82	82	85
E	76.3		72	65.5
		71		
F	65.5		70	58
A	48.7			
F	46.7		48	52,49
		50		
E	43.7		50	44

[a]Reference 19.
[b]Calculated from the structure factor $S(\mathbf{k},\omega)$ at 5 K. Only four peaks were clearly distinguished, which did not allow the assignment of the two low-frequency modes.
[c]From the calculated Raman spectrum of Fig. 4.
[d]From Refs. 37–39.

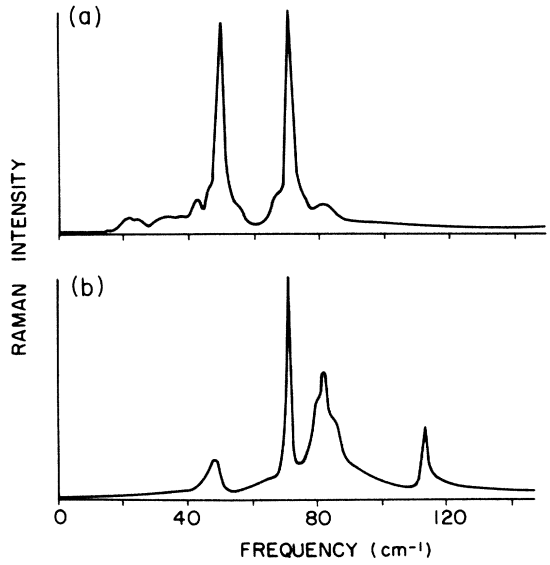

FIG. 4. Calculated Raman spectrum for (a) parallel and (b) perpendicular polarizations, based on constant-volume MD calculations for α-CO at 5 K. The peaks in the parallel polarization [panel (a)] refer to the two modes with symmetry E, while the peaks in the perpendicular polarization [panel (b)] are due to the four modes with symmetry F.

where the summation is over all molecules. The function A has the form $\frac{1}{2}(3z^2-1)$ for the E modes and xy for the F modes, and (x,y,z) are the components of a unit vector directed along the CO bond.

Results obtained at 5 K are shown in Fig. 4 for both the parallel [Fig. 4(a)] and the perpendicular [Fig. 4(b)] polarized scattering. The parallel components display two peaks, corresponding to the E modes, while the perpendicular component shows four peaks corresponding to the four F bands. In constructing these spectra, we have averaged over symmetry-equivalent components (xx, yy, and zz for the parallel polarization, and xy, xz, and yz for the perpendicular one).

At 30 K the calculated spectral lines are broadened, the increased background blurring the distinction between the peaks in the power spectrum. However, two maxima can be distinguished for the parallel polarization (at 55 and 70 cm^{-1}, respectively) and only three for the perpendicular one (two peaks at 72 and 105 cm^{-1}, and a broad structured band centered at 84 cm^{-1}). The correlation with experimental data is fairly good.

C. Orientational disordered hexagonal phase

We found no evidence to suggest that the instability in the cubic phase observed between 53 and 61 K was due to a transformation into an hexagonal phase. However, as mentioned in Sec. III it was possible to prepare the system in a stable hexagonal rotator phase. The corresponding atom-atom distribution functions $g_{\alpha\beta}(R)$ are shown in Fig. 3, for the run at 53 K. These distribution functions are more reminiscent of the liquid than of the ordered solid, due to the disorder in the molecular orientation.

However, the absence of self-diffusion at $T=53$ K, as measured by the time derivative of the center-of-mass displacement Δr,

$$D=\frac{1}{6}\frac{d\langle\Delta r^2\rangle}{dt}\ , \tag{5}$$

lead us to conclude that we had generated a plastic crystal. Actually, the disordering of the molecules was already evident during the constant-volume equilibration run at 39 K. The average inclination of the CO bond vector with respect to the crystal c axis was close to the "ideal" value of 54°44'. The increase in the molar volume on passing from the ordered cubic phase to the disordered hexagonal phase is no doubt due primarily to rotational motion.

D. The liquid

Above 60 K, both the cubic and hexagonal structures became unstable. Here, the MD cells deformed and were typically characterized by fluctuations of approximately 2% in their edge lengths and approximately 3% in their angles. One of the runs started from the hexagonal phase (V) and four (5–8) from the cubic phase produced liquids (Table IV).

The radial distribution functions, which are reported in Fig. 3 for the run at 71 K, are typical of a liquid state. Moreover, the system is now characterized by a finite self-diffusion coefficient D (see Table IV). In Fig. 5 the calculated values for D are compared with the experimental values.[40] In view of the large errors (approximately 30%) in the evaluation of D and the discrepancy between theory and experiment[45] in the molar volumes (recall Fig. 1), the agreement with experimental values for D is as good as could be expected. It should be noted that the molar volume and enthalpy of point V does not lie on the smooth curve determined by the other liquid points 5–8, shown in Figs. 1 and 2. Differences in system size (128:108), periodic boundary conditions (hcp:fcc), and potential truncation are likely responsible for this discrepancy.

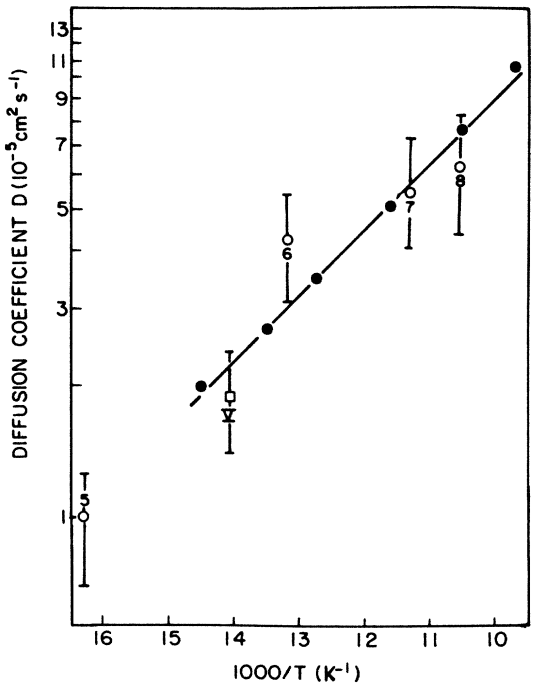

FIG. 5. Temperature dependence of the self-diffusion coefficient D of liquid CO (the experimental values are from Ref. 39) compared to the constant-pressure MD results (open circles, originating from the $P2_13$ structure, and square, originating from the hcp structure).

VI. CONCLUSIONS

Constant-pressure MD calculations for carbon monoxide have been performed, employing a potential model derived in part from LD calculations for an ordered α phase. The potential yields a stable antiferro ordered cubic structure up to approximately 53 K. The dynamical properties derived from MD calculations of low temperature are consistent with the findings from lattice-dynamics calculations.

We did not observe the cubic→hexagonal transition by simply heating at constant pressure. This was unfortunate, but not surprising: The simplest way to pass from the fcc to the hcp structure involves displacements of the molecules along the diagonal planes of the cubic lattice, and this (with a MD cell of only 108 molecules) is probably inhibited by the boundary conditions. Nevertheless, the model produces a stable plastic hexagonal phase, once the system is prepared as such (with $\Delta H\simeq 0.25$ kJ/mol relative to the α phase). In real CO the β phase exists over a rather limited temperature range, beyond which the system melts. We found that, starting from the cubic phase, the system reaches a region of instability at around 53 K, and above 60 K its behavior is that of a liquid. It is within this interval that the plastic hcp arrangement (still fairly stable) has an enthalpy lower than that of its "cubic" counterpart. We could speculate that the irregular behavior of the cubic phase denotes an attempt of the system to transform to the hexagonal phase, an attempt which is frustrated by the boundary conditions. Below 53 K our model accounts for both an ordered cubic and a plastic hexagonal phase, but, because of lower values of both the enthalpy and the molar volume, the fcc phase is probably the most stable of the two coexisting phases. Above 60 K the potential predicts a liquid (with $\Delta H\simeq 0.6$ kJ/mol relative to the β phase), no matter how the system was originally prepared.

Thus we may conclude that the proposed intermolecular potential for condensed CO, obtained from lattice-dynamics calculations on the α phase,[19] not only gives a satisfactory account of the dynamics of the cubic phase, but is semiquantitative in reproducing the phase diagram of condensed CO at low pressure. It may prove instructive to use this potential to explore the phase diagram of CO at higher pressures.[52]

ACKNOWLEDGMENTS

This work was supported by the National Sciences and Engineering Research Council (NSERC) of Canada and the Italian Minstero della Pubblica Instruzione. We are

indebted to R. G. Della Valle, and R. Righini, for numerous discussions, and to M. Moller for assistance during the MD calculations. One of us (P.F.F.) thanks NSERC for additional support through the International Scholar Exchange Program. Most of the calculations were performed on the AES Dorval Cray-1*S* computer through the use of a NSERC grant to another of us (M.L.K.).

---

*Permanent address: Dipartimento di Chimica, Università di Firenze, 9 via Gino Capponi, Florence 50121, Italy.

[1]S. Califano, V. Schettino, and N. Neto, *Lattice Dynamics of Molecular Crystals* (Springer, Berlin, 1981).

[2]S. L. Chaplot, K. R. Rao, and A. P. Roy, Phys. Rev. B **29**, 4747 (1984); S. L. Chaplot and K. R. Rao, J. Phys. C **16**, 3045 (1983).

[3]P. F. Fracassi, M. L. Klein, and R. G. Della Valle, Can. J. Phys. **62**, 54 (1984).

[4]K. H. Michel and J. Naudts, J. Chem. Phys. **67**, 547 (1977); **68**, 216 (1978).

[5]R. Lynden Bell, M. L. Klein, and I. R. McDonald, Mol. Phys. **48**, 1093 (1983).

[6]A. P. J. Jansen, W. J. Briels, and A. van der Avoird, J. Chem. Phys. **81**, 3648 (1984); A. van der Avoird, W. J. Briels, and A. P. L. Jansen, *ibid.* **81**, 3658 (1984); W. J. Briels, A. P. L. Jansen, and A. van der Avoird, *ibid.* **81**, 4118 (1984).

[7]M. L. Klein and J. J. Weis, J. Chem. Phys. **67**, 217 (1977).

[8]D. G. Bounds, M. L. Klein, and G. N. Patety, J. Chem. Phys. **72**, 5348 (1980).

[9]M. L. Klein and I. R. McDonald, Chem. Phys. **72**, 383 (1982).

[10]H. C. Andersen, J. Chem. Phys. **72**, 2384 (1980).

[11]M. Parrinello and A. Rahman, Phys. Rev. Lett. **45**, 1196 (1980); J. Appl. Phys. **52**, 7182 (1981); J. Phys. (Paris) Colloq. **42**, C6-511 (1981).

[12]M. Parrinello, A. Rahman, and P. Vashishta, Phys. Rev. Lett. **50**, 1073 (1983).

[13]S. Nosé and M. L. Klein, J. Chem. Phys. **78**, 6928 (1983); Phys. Rev. Lett. **50**, 1207 (1983).

[14]R. W. Impey, M. L. Klein, and I. R. McDonald, J. Chem. Phys. **82**, 4690 (1985).

[15]N. Corbin, W. J. Meath, and A. R. Allnatt, Mol. Phys. **53**, 225 (1984).

[16]R. M. Berens and A. van der Avoird, J. Chem. Phys. **72**, 6107 (1980); T. Luty, A. van der Avoird, and R. M. Berens, *ibid.* **73**, 5305 (1980).

[17]M. S. H. Ling and M. Rigby, Mol. Phys. **51**, 855 (1984).

[18]R. LeSar, J. Chem. Phys. **81**, 5104 (1984); R. LeSar and R. G. Gordon, *ibid.* **78**, 4991 (1983).

[19]P. F. Fracassi and M. L. Klein, Chem. Phys. Lett. **108**, 359 (1984); P. F. Fracassi, R. Righini, R. G. Della Valle, and M. L. Klein, Chem. Phys. **96**, 361 (1985).

[20]G. A. Parker and R. T. Pack, J. Chem. Phys. **64**, 2010 (1976).

[21]F. Mulder, G. F. Thomas, and W. J. Meath, Mol. Phys. **41**, 249 (1980).

[22]B. L. Jhanwar and W. J. Meath, Chem. Phys. **67**, 185 (1982).

[23]J. Hoinkis, R. Ahlrichs, and H. H. Böhm, Int. J. Quantum Chem. **23**, 821 (1983).

[24]J. O. Clayton and W. F. Giaugue, J. Am. Chem. Soc. **54**, 2610 (1932).

[25]E. K. Gill and J. A. Morrison, J. Chem. Phys. **45**, 1985 (1966).

[26]J. C. Burford and G. M. Graham, Can. J. Phys. **47**, 23 (1969).

[27]H. Suga and S. Seki, Faraday Discuss. **69**, 221 (1980); T. Ataki, H. Suga, and H. Chihara, Chem. Lett. (Japan) 567 (1976).

[28]L. Vegard, Z. Phys. **61**, 183 (1930); **88**, 235 (1934).

[29]I. N. Krupskii, A. I. Prokhvatilov, A. I. Erenburg, and L. D. Yantsevich, Phys. Status Solidi A **19**, 519 (1973).

[30]K. R. Nary, P. L. Kuhns, and M. S. Conradi, Phys. Rev. B **26**, 3370 (1982).

[31]F. Li, J. Brookeman, A. Rigamonti, and T. A. Scott, J. Chem. Phys. **74**, 3120 (1981).

[32]J. Walton, J. Brookeman, and A. Rigamonti, Phys. Rev. B **28**, 4050 (1983).

[33]S.-B. Liu and M. S. Conradi, Phys. Rev. B **30**, 24 (1984).

[34]R. F. Curl, Jr., H. P. Hopkins, Jr., and T. A. Scott, J. Chem. Phys. **48**, 4064 (1968).

[35]M. W. Melhuish and R. L. Scott, J. Chem. Phys. **68**, 2301 (1964).

[36]B. C. Kohin, J. Chem. Phys. **33**, 882 (1960); T. Shinoda and H. Enokido, J. Phys. Soc. Jpn. **26**, 1353 (1969); D. A. Goodings and M. Henkelman, Can. J. Phys. **49**, 2898 (1971); B. Okray-Hall and H. M. James, Phys. Rev. B **13**, 3590 (1976).

[37]A. Anderson and G. E. Leroi, J. Chem. Phys. **45**, 4359 (1966).

[38]A. Ron and O. Schnepp, J. Chem. Phys. **46**, 3991 (1967).

[39]A. Anderson, T. Sun, and M. C. A. Donkersloot, Can. J. Phys. **48**, 2265 (1970).

[40]E. Fukushima, A. A. V. Gibson, and T. A. Scott, J. Chem. Phys. **71**, 1531 (1979).

[41]P. H. Gammon, H. Kiefte, and M. J. Clouter, J. Chem. Phys. **70**, 810 (1978).

[42]E. Fukushima, A. A. V. Gibson, and T. A. Scott, J. Chem. Phys. **66**, 4811 (1977).

[43]W. Press and A. Hüller, J. Chem. Phys. **68**, 4465 (1978).

[44]L. A. K. Staveley, J. Phys. Chem. Solids **18**, 46 (1961).

[45]J. Timmermans, *Physico-Chemical Constants of Pure Organic Compounds* (Elsevier, New York, 1950, 1965), Vols. I and II; C. L. Yaws, K. Y. Li, and C. H. Kuo, Chem. Eng. **81**, 115 (1974).

[46]B. P. Stoicheff, Can. J. Phys. **32**, 630 (1954).

[47]K. K. Kelley, U.S. Bur. Mines **34**, 383 (1935).

[48]D. Ceperley, in Proceedings of a Workshop on the Problem of Long Range Forces in the Computer Simulation of Condensed Media, Menlo Park, California, 1980 (unpublished).

[49]S. Murad and K. E. Gubbins, in *Computer Modeling of Matter,* edited by P. Lykos (American Chemical Society Symposium Series No. 86) (ACS, Washington, D.C., 1978), p. 62.

[50]R. W. Impey, S. Nosé, and M. L. Klein, Mol. Phys. **50**, 243 (1983).

[51]J. P. Ryckaert, C. Ciccotti, and J. C. Berendsen, J. Comp. Phys. **23**, 327 (1977).

[52]D. T. Cromer, D. Schiferl, R. LeSar, and R. L. Mills, Acta Crystallogr. Sect. C **39**, 1146 (1983); A. I. Katz, D. Schiferl, and R. L. Mills, J. Phys. Chem. **88**, 3176 (1984).